*Journal of Superconductivity, Vol. 5, No. 4, 1992*

# Magnetic Penetration Depth Measurements in Cuprate Superconductors

**Steven M. Anlage[1] and Dong-Ho Wu[1]**

*Received 16 April 1992*

We examine recent results on measurements of the magnetic penetration depth in cuprate superconductors, with particular emphasis on our results obtained with the microstrip and parallel-plate resonator techniques. The results show that the magnetic penetration depth temperature dependence in $YBa_2Cu_3O_{7-\delta}$ is not consistent with a simple scaled weak-coupled BCS temperature dependence. We present three classes of interpretations of these measurements, and how they relate to other experimental studies of the cuprates. Finally, these interpretations are discussed in terms of some theories of cuprate superconductivity.

**KEY WORDS:** Magnetic penetration depth; surface impedance; cuprate superconductors.

## 1. INTRODUCTION

One of the hallmarks of superconductivity is the diamagnetic response of a superconductor below its transition temperature $T_c$. The ability to spontaneously eliminate a static magnetic field from the bulk of the material (Meissner effect) clearly distinguishes superconductors from mere perfect conductors. However, the diamagnetic shielding currents never completely eliminate an applied magnetic field from the interior of a superconductor, even in the absence of pinning and in the limit of infinitesimal field strength. Shielding currents do not flow in a sheath of zero thickness, as in a perfect conductor, but over a finite depth below the surface. This length scale is the magnetic penetration depth $\lambda$. If the applied field varies at finite frequency, the superconducting condensate will not respond exactly in phase with the time-varying field, and thus some dissipative currents will flow along with the shielding currents. The degree to which these other currents flow is measured by the surface resistance $R_s$ of the superconductor. The penetration depth and surface resistance can be thought of in terms of the complex surface impedance, which for a flat and very thick ($t \gg \lambda$) superconductor is $Z = R_s + i\omega\mu_0\lambda$. The penetration depth and surface resistance can also be found from the complex conductivity $\sigma \equiv \sigma_1 - i\sigma_2$, which for good conductors is related to the surface impedance as $Z = [i\omega\mu_0/\sigma]^{1/2}$.

### 1.1. The Surface Impedance

Measurements of the surface impedance are important because they directly probe the response of the superconducting carriers and the quasiparticles. In particular, the detailed temperature dependence of the strength of the shielding currents in a superconductor are directly related to the existence, or absence, of a finite energy gap for quasiparticle excitations in the superconducting state. Conventional superconductors with a finite energy gap over their entire Fermi surface show an exponential decrease of the penetration depth and surface resistance at low temperatures. Unconventional superconductors with nodes in their energy gap show a polynomial dependence of the penetration depth at low temperatures because of the availability of quasiparticle states of arbitrarily small energy. In addition to the fundamental relation to the superconducting properties, surface impedance measurements are very surface sensitive, because the fields are limited to a few penetration depths of the surface.

[1]Center for Superconductivity Research, Physics Department, University of Maryland, College Park, Maryland 20742-4111.



0896-1107/92/0800-0395$06.50/0 

This also makes surface impedance measurements ideal for studying the "bulk" properties of thin films.

Many surface impedance measurements are performed at microwave frequencies for a number of reasons. First, sources with frequency stability of 1 part in $10^9$ are available off-the-shelf, allowing one to design very sensitive resonant measurements. Also, microwave sources are phase coherent, and this permits direct measurement of the complex impedance or conductivity of a sample. Third, because the surface resistance increases quadatically with frequency at low frequencies, the surface resistance of superconductors is in the micro-ohm to milli-ohm range at microwave frequencies. Such losses are easily measured by a variety of resonant and nonresonant techniques. Finally, the magnetic penetration depth is only weakly dependent on frequency as long as $\omega\tau \ll 1$, where $\tau$ is the quasiparticle lifetime, so measurements of $\lambda$ at microwave frequencies can be compared with those obtained by low-frequency or dc techniques.

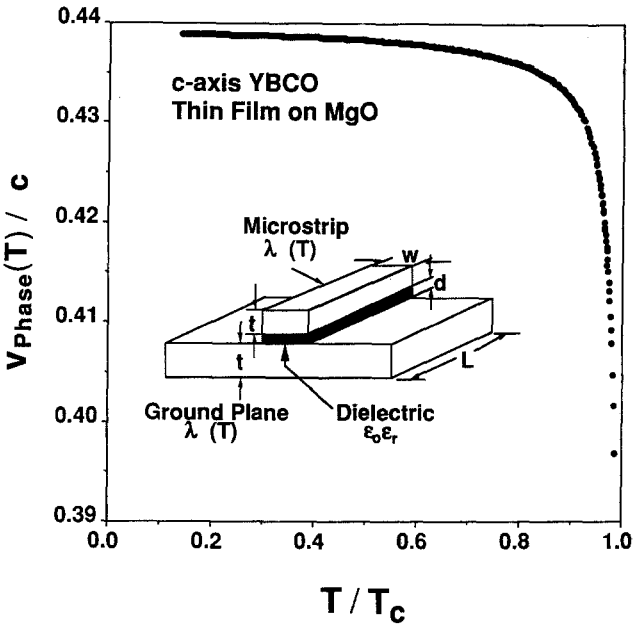


**Fig. 1.** Measured phase velocity vs. temperature for a flip-chip microstrip resonator composed of two $c$-axis YBCO films on MgO substrates. Inset shows the microstrip geometry and relevant length scales and dielectric properties used to determine the magnetic penetration depth in the superconducting films.

## 2. EXPERIMENTAL TECHNIQUES

### 2.1. Transmission Line Resonators

An ideal measurement of the surface impedance could be done in a resonant cavity in which all the electric and magnetic fields are enclosed by the sample of interest. Thus all the losses and inductances measured would be attributable only to superconducting surfaces. However, in practical measurements, it is often not possible to make a resonant cavity out of a single high-quality material, and alternative methods must be sought. In most alternative methods, the fields of the resonant mode must also exist inside a dielectric material, and some fields may escape from the region near the sample and radiate away. The microstrip, stripline and parallel-plate resonator techniques come progressively closer to the ideal situation. The basic idea of these transmission line resonator measurements is to deduce the penetration depth from a measurement of the phase velocity of a microwave signal propagating on a thin-film superconducting transmission line, and the surface resistance of the film is found from the $Q$ of the resonance.

In the particular case of a microstrip transmission line (see the inset of Fig. 1), the dependence of the measured phase velocity on the penetration depth in the thin film is given by [1–3]

$$\frac{v_{ph}(T)}{c} = \frac{1/\sqrt{\varepsilon_{eff}}}{\sqrt{1+2[\lambda(T)/d]\coth(t/\lambda(T))}} \quad (1)$$

where $d$ is the dielectric thickness, $\varepsilon_{eff}$ is the effective relative dielectric constant, the phase velocity is related to the measured resonant frequency by $v_{ph} = 2Lf_n/n$, where $L$ is the length of the resonator and $n$ is the harmonic number, and both films in the transmission line are of thickness $t$ and have penetration depth $\lambda(T)$. With this technique it is possible to measure changes in $\lambda$ of less than 1 Å, an order of magnitude better than other techniques used to date [3]. If radiation and dielectric losses are not significant, the surface resistance can be found from the $Q$ of the resonance through $R_s = \pi\mu_0 f/Q$, where $f$ is the resonant frequency.

In a typical experiment, two identically prepared superconducting films on separate substrates are used to make a flip-chip parallel-plate transmission line resonator by sandwiching a thin dielectric sheet (e.g., Teflon FEP) between the films and clamping the whole assembly. The shielding currents for the propagating mode flow entirely in the direction parallel to the surface of the film. The measurements are performed at excitation levels for which the data are independent of the applied microwave power. Representative data for a pair of $c$-axis $YBa_2Cu_3O_{7-\delta}$ (YBCO) films is shown in Fig. 1.

### 2.2. Other Resonant Techniques

Many groups employ normal metal [4] and superconducting [5] microwave cavities for resonant measurements of the magnetic penetration depth. The cavities are typically right cylinders, and are excited in the $TE_{011}$ mode. This mode generates strong azimuthal surface currents on the flat end-walls of the cavity. The superconducting sample is made into one of the flat end-walls, and the penetration depth is obtained from the resonant frequency shift with temperature, after a background subtraction is done. Alternatively, the sample can be placed in another high-field region at the center of the cavity [5].

Schawlow and Devlin measured the magnetic penetration depth of cylindrical samples by wrapping a tank oscillator inductor coil around the sample and monitoring the resonant frequency of the circuit as a function of temperature [6]. This technique has been used successfully with the cuprate materials [5, 7], where the temperature and field dependence of $\lambda$ in YBCO crystals has been measured.

Another variation of the resonant technique has been demonstrated by Bonn *et al.* They have employed a split-ring resonator to measure the surface resistance of small superconducting samples [8], including cuprate single crystals [9].

All of these techniques measure the quality factor $Q$ and resonant frequency shift $\delta\omega$ to extract $R_s$ and $\lambda$ using the relations $R_s = \Gamma(1/Q - 1/Q_{\text{cavity}})$ and $\delta\lambda = \gamma\delta\omega$, where $\Gamma$ and $\gamma$ are geometrical factors determined by the size of the cavity and sample, along with the sample position.

### 2.3. Nonresonant Techniques

Muon spin rotation has proven to be an invaluable probe of the magnetic penetration depth in superconductors. It is unique in that it measures the penetration depth in the bulk of the material, rather than just at the surface. This greatly reduces the need to prepare very high quality and stable surfaces of the material, but brings in other complications with regard to the homogeneity of doping in the bulk. Measurements at sufficiently high fields can largely overcome this problem though. These measurements have revealed the existence of a correlation in the cuprates between the superconducting transition temperature and the muon spin relaxation rate at zero temperature [10], which is directly proportional, in the clean, local limit, to $n_s/m^*$ of the superconducting condensate. As far as the temperature dependence of the penetration depth is concerned, most of the results on cuprates are consistent with the two-fluid temperature dependence, but more detailed examination of the temperature dependence does not seem justified in light of the large error bars on the data, and the time required to collect a decay-product histogram.

Transmission measurements through thin films [11] and thinned single crystals [12] are a very sensitive method of measuring the magnetic penetration depth. In the low-temperature limit where $\sigma_2 \gg \sigma_1$, the transmission coefficient of a superconducting film is proportional to the fourth power of the penetration depth: $T \sim 1/\sigma_2^2 \sim \lambda^4$. These measurements can be performed at microwave [13], millimeter wave, [14] and far-infrared frequencies [15, 16].

Picosecond pulse propagation on superconducting transmission lines can be used to measure the surface resistance and reactance of the films making up the transmission line [17–19]. An innovative variation is to study the transmission and reflection of picosecond pulses through the superconducting films [20].

The mutual inductance technique has been used to study the Kosterlitz–Thouless transition in thin superconducting films [21], as well as the effects of electric fields on the electrodynamic properties of cuprate thin films [22].

Magnetic neutron scattering from flux-line arrays is also being used to measure the penetration depth in thin-film superconductors [23, 24].

## 3. MATERIALS ISSUES

Historically, the best understood relationship between microstructure and surface impedance measurements is that for niobium. The virgin surface of niobium is very quickly oxidized in air. Surface analysis reveals that oxygen diffuses into niobium, forming a continuous solid solution out to roughly NbO [25]. At higher concentrations, compounds such as $Nb_2O_5$ form. It is known that the substoichiometric material $NbO_x$ is superconducting with $T_c$'s below those of bulk Nb.

It is believed that the oxides of Nb form islands near the surface of Nb whose dimensions are comparable to both the magnetic penetration depth ($\lambda_L =$ 390 Å) and the clean limit coherence length ($\xi_0 =$ 380 Å). When shielding currents flow near the surface of a contaminated Nb surface, they encounter islands of material which are either nonsuperconducting, weakly superconducting, or insulating. The dimensions of these islands are comparable to the coherence

length, hence they give rise to weak-link tunnel structures for the shielding currents. Associated with these tunnel structures are normal-metal tunnel currents which dissipate power, and an enhanced inductance, which increases the measured penetration depth. It is found experimentally that although the surface impedance of Nb follows the predictions of BCS theory at temperatures just below $T_c$, there is a temperature below which the surface resistance fails to follow the BCS prediction. The resulting residual resistance is associated with the imperfections of the Nb surface, and much effort has been devoted to mitigating their effect.

Because of their short coherence lengths, larger penetration depths, and complicated crystal structure, cuprate superconductors are expected to be even more sensitive to materials imperfections. In our $\lambda(T)$ measurements we choose to concentrate on the YBCO films on MgO substrates because it is known from transport studies that they have better normal state properties than those on yttria-stabilized zirconia or $LaAlO_3$ (26, 27]. In addition, the best films on MgO studied here have a normal state resistivity at 100 K of 60 $\mu\Omega$cm [26], an rf residual loss of 16 $\mu\Omega$ at 10 GHz, 4.2 K [28] an absolute value of $\lambda(0) \approx 1400$ Å [26], and a low abundance of high-angle grain boundaries [28], making them among the best high-$T_c$ films available. As already mentioned, like all films they are highly twinned and in our measurements the shielding currents in $c$-axis films will flow roughly equally along the $a$- and $b$-directions. Nevertheless the transport properties of these YBCO/MgO films are comparable to single crystals and their rf properties are in fact as good or superior.

## 4. DATA

### 4.1. Microstrip Transmission Line Resonators

We choose to first examine the raw data at low temperatures. For thick films ($t > 3\lambda(0)/2$) one finds, from Eq. (1),

$$\left(\frac{c}{v_{ph}(T)}\right)^2 \cong \varepsilon_{eff}\left[1+\frac{2\lambda(T)}{d}\right]$$

The temperature dependence of the right-hand side of this equation is solely that of the magnetic penetration depth [3]. Plots of the raw data vs. temperature in this form show better fits to an exponential temperature dependence: $\Delta\lambda(T) \sim T^{-1/2} e^{-\Delta(0)/k_B T}$, rather than a power-law temperature dependence: $\Delta\lambda(T) \sim (T/T_c)^n$. It is found that $2\Delta(0)/k_B T_c \sim 1$–2 and $n \sim 2.5$–3 depending on the films studied [29].

Because it is not possible to uniquely determine a zero-temperature baseline for the measured phase velocity, we must extract $\lambda(T)$ from the phase velocity data by fitting the data to an assumed theoretical temperature dependence self-consistently [2, 3]. The parallel-plate resonator data for a sputtered Nb film can be self-consistently fitted very well with a BCS temperature dependence over the entire temperature range of the measurement using a single energy gap[2] with a value of $2\Delta(0)/k_B T_c \approx 3.6$. The value of the gap is similar to that obtained by tunneling, which gives $2\Delta(0)/k_B T_c = 3.8$ for Nb [31]. The value of $\lambda(0)$ in the sputtered Nb film is found to be approximately 535 Å.

In the case of our YBCO/MgO films, we find that the temperature dependence of $\lambda$ cannot be self-consistently fitted to a BCS temperature dependence derived from a single energy gap over the entire temperature range from $T_c$ to low temperatures [2]. The low-temperature data can be fitted to a BCS temperature dependence with a single gap of $2\Delta(0)/k_B T_c = 1$–2.5,[3] depending on the specific film studied [2]. By examining the entire temperature dependence of $(\lambda(0)/\lambda(T))^2$, we find that the high-temperature ($0.65T_c$ to $0.98T_c$) data best fits a single-gap BCS temperature dependence with an effective $2\Delta(0)/k_B T_c = 4.5 \pm 0.25$ [2]. This is in good agreement with measurements of $\lambda(T)$ restricted to this same temperature range in single crystal YBCO [32] where it was found that a single-gap BCS fit yields $2\Delta(0)/k_B T_c = 4.3$. Thus, it seems that the electrodynamic response of the cuprate superconductors provides additional evidence for large $2\Delta(0)/k_B T_c$ in these materials; although lacking any direct evidence for the validity of scaled weak-coupled, isotropic BCS theory, it is not clear how accurate the inferred values of $2\Delta(0)/k_B T_c$ actually are.

[2]The BCS $\lambda(T)$ is calculated using an isotropic scaled weak-coupling theory by the method of J. Halbritter [30]. By varying $2\Delta(0)/k_B T_c$ with this method, one can examine the effects of strong coupling without resorting to more elaborate theories. Parameters for Nb are $T_c = 9.0$ K, $l_{MFP} = 130$ Å, $\lambda_L = 390$ Å, and $\xi_0 = (2/\pi)\xi_F = 380$ Å. Parameters chosen for $YBa_2Cu_3O_{7-\delta}$ are $\xi_F = (\pi/2)\xi_0 = 15$ Å, $\lambda_L = 1400$ Å, $l_{MFP} = 100$ Å, and $T_c = 90$ K.

[3]Early measurements of $\lambda(T)$ in the microstrip resonator geometry were influenced by a temperature-dependent dielectric constant associated with the presence of helium vapor. This led to somewhat enhanced estimates of the magnitude of the low-temperature energy gap. The data discussed here has been gathered in vacuum and is not influenced by the helium vapor effect. Our conclusions in [2] regarding exponential vs. power-law temperature dependence of $\lambda(T)$ remain the same.

It would appear that experimentalists agree that there is a non-BCS temperature dependence for the penetration depth, at least in thin films and fine powders. Measurements of the magnetic penetration depth in YBCO films by Fiory, using the mutual inductance technique, show results similar to ours [33]. The results of Pond *et al.* [34] on integrated microstrip transmission line resonators are also strikingly similar to our own. Finally, the magnetic susceptibility data of Gantmakher on ultrafine powders of YBCO show similar behavior [35]. There remains an open question about how $\lambda(T)$ behaves at low temperatures in high-quality twinned and untwinned single crystals of the cuprates.

## 5. MODELS

We consider three broad classes of interpretations that have arisen to explain the magnetic penetration depth measurements in the cuprates.

### 5.1. Extrinsic (Materials Limited) Surface Impedance

Based on the lessons learned from materials issues and the surface impedance of niobium, and the fact that cuprate materials will be even more microstructure sensitive, some researchers believe that virtually all measurements of the surface impedance published to date on the cuprates have been strongly influenced by extrinsic materials effects. Quantitative models based on this idea have centered around a two-fluid model [28, 36, 37], the weak link model [38, 39], and vortex–antivortex generation at defects [40].

In the two-fluid model, the superconductor is assumed to have a nonzero density of unpaired electrons, even at zero temperature. It is found that this density must be on the order of 25% of the zero-temperature superfluid density to account for the residual surface resistance measured in YBCO thin films [28, 36]. The source of these unpaired electrons was once thought to be the "nonsuperconducting" doping layers between the Cu–O planes, but their density is too high to explain the observed residual losses. Now it is believed that disordered regions of the doping layers or Cu–O planes are responsible.

The weak-link model posits the existence of an array of tunnel barriers for shielding currents flowing near the surface of the cuprate materials. These tunnel barriers may arise at grain boundaries, twin boundaries, or possibly in oxygen-deficient regions. The weak links have a tunneling critical current density $J_c(T)$, a normal leakage current which gives rise to a resistance $R_N$, and a characteristic spacing $a$. The measured surface resistance and magnetic penetration depth, in the small-grain limit $a \ll \lambda$, is then given by [38]

$$R_s(T, \omega) = \omega \mu_0 \lambda_{\text{eff}}(T) \times \frac{1}{2} \frac{\lambda_{\text{eff}}^2(T) - \lambda_{\text{sc}}^2(T)}{\lambda_{\text{eff}}^2(T)} \frac{h\omega}{4\pi I_c R}$$

$$\lambda_{\text{eff}}(T) = \sqrt{\lambda_{\text{sc}}^2(T) + \frac{\Phi_0}{2\pi\mu_0 a J_c(T)}}$$

where $\lambda_{\text{sc}}(T)$ is the penetration depth of a perfect superconducting grain. This model also qualitatively explains the magnetic field dependence of the surface impedance [41, 42]. Excellent fits to the measured $\lambda(T)$ [2] and $R_s(T)$ [28] of YBCO films were obtained with the same set of parameter values. Also, the frequency dependence of this model was tested through successful fits to $R_s$ (4.2 K, 10 GHz) and the far-infrared absorption of YBCO films [37].

The third model centers on nonsuperconducting defects at the surface of the material. When strong shielding currents flow around these defects, a vortex–antivortex pair can be created [40]. The vortices will be pinned almost immediately, and they will contribute to the screening. The length scale over which they shield is the pinning penetration depth $\lambda_p$. The temperature dependence of $\lambda_p$ is simply that of the restoring force of the pinning site, which scales with the thermodynamic critical field: $H_c(T) \approx H_c(0)(1-(T/T_c)^2)$. This pinning penetration depth temperature dependence was seen in YBCO films in which defects were intentionally introduced, but not in more nearly perfect films [40]. These pinned vortices will also contribute a residual surface resistance.

### 5.2. Finite-Gap Interpretation

If a finite energy gap exists over the entire Fermi surface of a superconductor, one expects the surface impedance to show an exponential drop at low temperatures in the clean local limit: $\lambda(T)/\lambda(0) - 1 \sim T^{-1/2} e^{-\Delta(0)/k_B T}$, $R_s(T) \sim e^{-\Delta(0)/k_B T}$, where $\Delta(0)$ is the smallest energy gap on the Fermi surface. Such behavior is seen in many of the $s$-wave superconductors, except at the lowest temperatures where extrinsic effects eventually dominate. Our own measurements of $\lambda(T)$ below $T_c/2$ are consistent with the finite-gap interpretation if one takes values of $2\Delta(0)/k_B T_c \sim 1$–2.5. Until recently, all measurements of $R_s(T)$ in the cuprates either show a large residual

resistance which sets in around 75% of $T_c$, [43] or had losses which were below the resolution limit of the measurement technique. No evidence for an exponential decay of the surface resistance in any cuprate material was seen until 1991 [44, 45]. As with our penetration depth measurements, the energy gap deduced is quite small: $2\Delta(0)/k_BT_c \sim 0.8$. Hence, at least a subset of the data on the surface impedance of YBCO is consistent with a finite energy gap over the entire Fermi surface.

It has also been suggested that the YBCO material may be a two-band superconductor, with a large energy gap associated with the planes, and a smaller, proximity-induced, gap in the chain layers [46]. Similar theories posit that the cuprates are intrinsic superconductor/normal superlattices [47–49] or have a highly anisotropic, but everywhere nonzero, energy gap [50]. For this class of theories, measurements of $\lambda(T)$ and $R_s(T)$ would reflect a whole range of $2\Delta(0)$ values, with the smallest gaps dominating at low temperatures. This is indeed consistent with measurements. The existence of an anisotropic or multiple superconducting gaps is consistent with a variety of other observations on the cuprates, including tunneling measurements [51], NMR [52] and Raman scattering in $Y_2Ba_4Cu_8O_{10}$ [53]. However, detailed fits of a simple two-gap model to penetration-depth measurements in YBCO films produced results for the ratio $m^*/n_s$ for the two systems in conflict with IR reflectivity data [2]. However, this discrepancy may be due to the naive belief that plane and chain conductivities are uncoupled and independent, or to poor oxygenation of the de-twinned crystal used in the IR experiment.

### 5.3. Nodes in the Energy Gap

The existence of a large residual surface resistance in the cuprates, and the fact that many $\lambda(T)$ measurements on YBCO can be fitted to the "gapless superconductor" temperature dependence $\lambda(T) = \lambda(0)/(1-(T/T_c)^2)^{1/2}$ [54], has led some to conclude that the cuprates have, at the very least, a node in the superconducting energy gap. Other data are in agreement with this interpretation, such as the existence of nonzero absorptivity at all frequencies in the far-infrared for electric fields polarized along both the *a*- and *b*-axes of de-twinned YBCO single crystals [55].

Many theories of cuprate superconductivity are based on the assumption that antiferromagnetic spin fluctuations are responsible for the superconducting pairing mechanism in the cuprates. Such theories favor paired states with *d*-wave symmetry, and consequently predict nodes in the energy gap for certain directions in *k*-space [56]. Other theories, such as the modified *s*-wave theory [57], predict a radial node in the energy gap, and a polynomial temperature dependence for the penetration depth at low temperatures. A group-theoretic analysis of the pairing states in YBCO led to the conclusion that the penetration depth should have a $\Delta\lambda_{ab}(T) \sim T$ dependence at low temperatures [58]. Also, strong-coupling BCS theory predicts a polynomial temperature dependence in $\lambda(T)$ [59].

Self-consistent fits of our microstrip and parallel plate resonator data to $\lambda(T) = \lambda(0)/(1-(T/T_c)^2)^{1/2}$ have been performed and provide a fairly good description of our data, although the *c*-axis data deviates away from the fit at low temperatures. However, it was noted that this temperature dependence fits the *a*-axis YBCO film data better than that of the *c*-axis film data (see Fig. 2). The *a*-axis films are known to contain at least three different kinds of grain boundaries [60], one of which forces the currents to flow from the *ab* planes of one grain into the *c*-axis direction of the neighboring grain. These films also have reduced $T_c$'s compared to *c*-axis films. Hence it is possible that the polynomial temperature dependence of the penetration depth in *a*-axis films is due to shielding currents flowing along the *c*-direction, or to weak links formed at one or more of the three types of grain boundaries in the *a*-axis films.

Attempts have recently been made to extract the quasiparticle scattering rate, $1/\tau(T)$, from measurements of the surface impedance below $T_c$ [9, 20]. Bonn *et al.* found an exponentially decreasing scattering rate below $T_c$, but had to assume (in the context of a two-fluid model) that the normal fraction followed a polynomial temperature dependence: $x_n(T) \sim (T/T_c)^2$. This interpretation may be consistent with the marginal Fermi liquid phenomenology, which proposes that the excitations which scatter the quasiparticles in the cuprates will themselves develop a gap below $T_c$ [61].

## 6. CONCLUSIONS

We believe that there is some convergence of experimental results on the temperature dependence of the magnetic penetration depth in cuprate superconductors. The temperature dependence of $\lambda$ does not follow a simple scaled-weak-coupled, single-gap

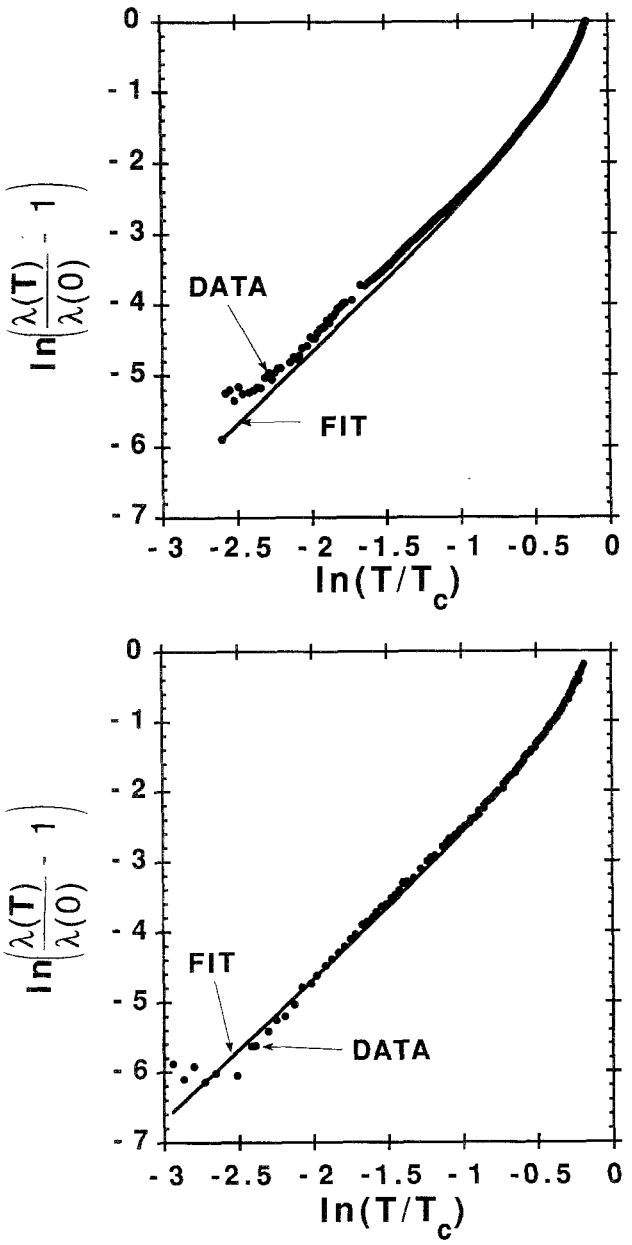


Fig. 2. Plot of $\ln(\lambda(T)/\lambda(0)-1)$ vs. $\ln(T/T_c)$ for data self-consistently fitted to the temperature dependence: $\lambda(T)=\lambda(0)/(1-(T/T_c)^2)^{1/2}$. Also shown is the theoretical temperature dependence itself plotted as a solid line. (a) Data for *c*-axis YBCO films on MgO substrates, (b) data for *a*-axis oriented films on $LaAlO_3$ substrates. Note that a better self-consistent fit is obtained for the *a*-axis data than for the *c*-axis data.

BCS temperature dependence. Instead, many interpretations of $\lambda(T)$ are possible, including extrinsic weak-link effects, an everywhere nonzero but anisotropic energy gap, or possibly a state with nodes or lines of nodes in the energy gap. Yet, it should be noted that the weak-link model is quantitatively consistent with the temperature, frequency, and magnetic field dependencies of the surface impedance of $YBa_2Cu_3O_7$ films. Further experimental work on materials of higher quality and known microstructure are required to fully understand the surface impedance of the cuprates.

## ACKNOWLEDGMENTS

One of us (S.M.A.) would like to acknowledge the contributions of the Geballe-Beasley-Kapitulnik group at Stanford University to this work. In particular Brian Langley, Z. Ma and Howard Snortland are acknowledged for their contributions. This work is supported by the State of Maryland and the NSF Division of Materials Research.

## REFERENCES

1. S. M. Anlage, B. W. Langley, H. J. Snortland, C. B. Eom, T. H. Geballe, and M. R. Beasley, *J. Supercond.* **3**, 311 (1990).
2. S. M. Anlage, B. W. Langley, G. Deutscher, J. Halbritter, and M. R. Beasley, *Phys. Rev. B* **44**, 9764 (1991).
3. B. W. Langley, S. M. Anlage, R. F. W. Pease, and M. R. Beasley, *Rev. Sci. Instrum.* **62**, 1801 (1991).
4. L. Drabeck, K. Holczer, G. Grüner, J. J. Chang, D. J. Scalapino, A. Inam, X. D. Wu, L. Nazar, and T. Venkatesan, *Phys. Rev. B* **42**, 10202 (1990).
5. S. Sridhar and W. L. Kennedy, *Rev. Sci. Instrum.* **59**, 531 (1988).
6. A. L. Schawlow and G. E. Devlin, *Phys. Rev.* **113**, 120 (1959).
7. D.-H. Wu and S. Sridhar, *Phys. Rev. Lett.* **65**, 2074 (1990).
8. D. A. Bonn, D. C. Morgan, and W. N. Hardy, *Rev. Sci. Instrum.* **62**, 1819 (1991).
9. D. A. Bonn, P. Dosanjh, R. Liang, and W. N. Hardy, *Phys. Rev. Lett.* **68**, 2390 (1992).
10. Y. J. Uemura *et al.*, *Phys. Rev. Lett.* **66**, 2665 (1991).
11. J. Ceremuga, Z. Ma, M. R. Beasley, R. C. Taber, B. Langley, and B. Cole, presented at the International Superconducting Electronics Conference, Glasgow, 1991.
12. L. Forro *et al.*, *Phys. Rev. Lett.* **65**, 1941 (1990).
13. C. S. Nichols, N. S. Shiren, R. B. Laibowitz, and T. G. Kazyaka, *Phys. Rev. B* **38**, 11970 (1988).
14. W. Ho, P. J. Hood, W. F. Hall, P. Kobrin, A. B. Harker, and R. E. DeWames, *Phys. Rev. B* **38**, 7029 (1988).
15. F. Gao *et al.*, *Phys. Rev. B* **43**, 10383 (1991).
16. K. Karrai *et al.*, *Phys. Rev. Lett.* **69**, 355 (1992).
17. W. J. Gallagher, C.-C. Chi, I. N. Duling, D. Grischkowsky, N. J. Halas, M. B. Ketchen, and A. W. Kleinsasser, *Appl. Phys. Lett.* **50**, 350 (1987).
18. D. R. Dykaar, R. Sobolewski, J. M. Chwalek, J. F. Whitaker, T. Y. Hsiang, G. A. Mourou, D. K. Lathrop, S. E. Russek, and R. A. Buhrman, *Appl. Phys. Lett.* **52**, 1444 (1988).
19. M. C. Nuss, P. M. Mankiewich, R. E. Howard, B. L. Straughn, T. E. Harvey, C. D. Brandle, G. W. Berkstresser, K. W. Goossen and P. R. Smith, *Appl. Phys. Lett.* **54**, 2265 (1989).
20. M. C. Nuss, K. W. Goossen, P. M. Mankiewich, M. L. O'Malley, J. L. Marshall, and R. E. Howard, *IEEE Trans Magn.* **MAG-27**, 863 (1991); M. C. Nuss, P. M. Mankiewich, M. L. O'Malley, E. H. Westerwick, and P. B. Littlewood, *Phys. Rev. Lett.* **66**, 3305 (1991).

21. A. T. Fiory, A. F. Hebard, P. M. Mankiewich, and R. E. Howard, *Appl. Phys. Lett.* **52**, 2165 (1988).
22. A. T. Fiory *et al.*, *Phys. Rev. Lett.* **65**, 3441 (1990).
23. R. Felici, J. Penfold, R. C. Ward, E. Olsi, and C. Matacotta, *Nature* (*London*) **329**, 523 (1987).
24. H. Zhang, J. W. Lynn, C. F. Majkrzak, S. K. Satija, C. J. Lobb, and J. H. Kang, preprint (1992).
25. J. Halbritter, *J. Less-Common Met.* **139**, 133 (1988).
26. S. M. Anlage *et al.*, in *Physical Phenomena in Granular Materials*, G. D. Cody, *et al.*, eds., MRS Symposia Proceedings No. 195 (Materials Research Society, Pittsburgh, 1990).
27. C. B. Eom *et al.*, *Appl. Phys. Lett.* **55**, 595 (1989); C. B. Eom *et al.*, *Physica C* **171**, 354 (1990).
28. S. S. Laderman *et al.*, *Phys. Rev. B* **43**, 2922 (1991).
29. Z. Ma and M. R. Beasley, Private communication, 1992.
30. J. Halbritter, *Z. Phys.* **266**, 209 (1974); *Externer Ber., Kenforschungszentrum Karlsruhe* **3**, 70–76 (1970).
31. R. F. Broom and P. Wolf, *Phys. Rev. B* **16**, 3100 (1977).
32. S. Sridhar, D.-H. Wu, and W. Kennedy, *Phys. Rev. Lett.* **63**, 1873 (1989).
33. A. Fiory, Bull. *Am. Phys. Soc.* **37**, 779 (1992).
34. J. M. Pond, K. R. Carroll, J. S. Horowitz, D. B. Chrisey, M. S. Osofsky, and V. C. Cestone, *Appl. Phys. Lett.* **59**, 3033 (1991).
35. V. F. Gantmakher, N. I. Golovko, I. G. Naumenko, A. M. Neminsky, and A. V. Petinova, *Physica C* **171**, 223 (1990).
36. G. Müller, N. Klein, A. Brust, H. Chaloupka, M. Hein, S. Orbach, H. Piel, and D. Reschke, *J. Supercond.* **3**, 235 (1990).
37. D. Miller *et al.*, *Appl. Phys. Lett.* **59**, 2326 (1991).
38. T. L. Hylton and M. R. Beasley, *Phys. Rev B* **39**, 9042 (1989).
39. G. Deutscher and O. Entin-Wohlman, *J. Phys. C* **10**, L433 (1977).
40. A. F. Hebard, A. T. Fiory, M. P. Siegal, J. M. Phillips, and R. C. Haddon, *Phys. Rev. B* **44**, 9753 (1991).
41. J. Halbritter, *J. Appl. Phys.* **68**, 6315 (1990).
42. J. Halbritter, *J. Appl. Phys.* **71**, 1 (1992).
43. R. C. Taber, *Rev. Sci. Instrum.* **61**, 2200 (1990).
44. N. Klein *et al.*, *Physica C* **185–189**, 1777 (1991).
45. N. Klein *et al.*, *J. Supercond.* **5**, (1992); N. Klein *et al.*, these proceedings; G. Müller *et al.*, these proceedings.
46. V. Z. Kresin, S. A. Wolf, and G. Deutscher, *Physica C* **191**, 9 (1992).
47. M. Tachiki, S. Takahashi, F. Steglich, and H. Adrian, *Z. Phys. B* **80**, 161 (1990).
48. L. N. Bulaevskii and M. V. Zyskin, *Phys. Rev. B* **42**, 10230 (1990).
49. A. I. Buzdin, V. P. Damjanovic, and A. Yu. Siminov, *Phys. Rev. B* **45**, 1 (1992).
50. R. A. Klemm and S. H. Liu, *Phys. Rev. B* **44**, 7526 (1991).
51. J. M. Valles *et al.*, *Phys. Rev. B* **44**, 11986 (1991).
52. Barrett *et al.*, *Phys. Rev. B* **41**, 6283 (1990).
53. E. T. Heyen, M. Cardona, J. Karpinski, E. Kaldis, and S. Rusiecki, *Phys. Rev. B* **43**, 12958 (1991).
54. A. Abrikosov and L. P. Gor'kov, *Sov. Phys. JETP* **12**, 1243 (1961).
55. T. Pham, H. D. Drew, S. H. Moseley, and J. Z. Liu, *Phys. Rev. B* **41**, 11681 (1990).
56. P. Monthoux, A. V. Balatsky, and D. Pines, *Phys. Rev. Lett.* **67**, 3448 (1991).
57. F. Mila and E. Abrahams, *Phys. Rev. Lett.* **67**, 2379 (1991).
58. J. Annett, N. Goldenfeld, and S. R. Renn, *Phys. Rev. B* **43**, 2778 (1991).
59. J. Rammer, personal communication (1991).
60. C. B. Eom, A. F. Marshall, S. S. Laderman, R. D. Jacowtz, and T. H. Geballe, *Science* **249**, 1549 (1990).
61. E. J. Nicol and J. P. Carbotte, preprint, 1992.